The American Association of Petroleum Geologists Bulletin
V. 71, No. 1 (January 1987), P. 17-28, 9 Figs., 5 Tables

Fracture Development and Mechanical Stratigraphy of Austin Chalk, Texas[1]

KEVIN CORBETT,[2] MELVIN FRIEDMAN,[3] and JOHN SPANG[3]

ABSTRACT

The mechanical stratigraphy of the Upper Cretaceous Austin Chalk is established from study of fracture intensity along its outcrop trend from Dallas to San Antonio and westward to Langtry, Texas, and in the subsurface from study of cores and/or fracture identification logs from 30 wells. Three mechanical-stratigraphic units are recognized: (1) an upper, fractured massive chalk corresponding to the Big House Chalk Member; (2) a middle, ductile chalk-marl corresponding to the Dessau Chalk and Burditt Marl Members; and (3) a lower, fractured massive chalk corresponding to the Atco Chalk Member.

Representative samples from the three mechanical-stratigraphic units were experimentally shortened, dry, at 10, 17, 34, and 70 MPa confining pressure, at 24°C, and at a strain rate of 2.5×10^{-4} sec^{-1} to determine if the relative mechanical behavior observed at the surface could be extrapolated into the subsurface at different simulated burial depths. The experimentally determined ductilities parallel those determined from outcrop and subsurface studies. Multiple linear regression analysis indicates that porosity is most strongly correlated with fracture strength. Smectite-content has the second strongest correlation. For low-porosity specimens (9-13.5%), the strength of specimens with 4% smectite is reduced 30-42% compared to specimens with no smectite. The coefficient of internal friction at 17 MPa confining pressure decreases from 1.66 to 0.61 as smectite content increases from 0 to 4%.

SEM photomicrographs of undeformed specimens show that smectite and other clays are distributed as large (30 μm), discrete, amorphous, concentrated masses throughout the chalk. They are comminuted along the induced fracture surfaces where their grain size is 0.5 μm or less. These observations suggest that smectite acts as a "soft-inclusion," localizing shear failure and correspondingly weakening the material.

INTRODUCTION

Recent drilling activity in the Austin Chalk peaked with the discovery of prolific oil production in the Giddings field, Lee and Burleson Counties, Texas. The key to successful exploration in this chalk play has been to predict where natural fracturing is abundant. To enhance this prediction, we herein report on: (1) the number and nature of mechanical units in the Austin Chalk, as determined from outcrop fracture intensity, and how these mechanical units relate to the established stratigraphy, i.e., to establish the mechanical stratigraphy; (2) the relative mechanical behavior (brittle-ductile transition) of the mechanical-stratigraphic units through experimental rock deformation; and (3) the relation of this behavior to intrinsic rock properties such as composition, porosity, permeability, and texture.

The approach is threefold. First, we studied fracture intensity along the outcrop trend from Dallas southwest to Lozier Canyon, 32 km west of Langtry, to determine the number and nature of mechanical units present and their relationship to the established stratigraphy, thus defining the mechanical stratigraphy. Next, we studied the subsurface using cores and Fracture Identification Logs (FIL)[4] to confirm the presence in the subsurface of the mechanical units identified in outcrop. Finally, we experimentally deformed representative samples of each mechanical unit to delineate their relative mechanical behavior and to correlate this behavior with intrinsic rock properties such as porosity, permeability, composition, and texture, by means of multiple linear regression analysis.

GEOLOGIC SETTING

Regional geology, sedimentology, diagenesis, and stratigraphy of the Austin Chalk have been given elsewhere (Roemer, 1852; Hill, 1887; Weeks, 1945; Durham, 1957; Murray, 1961; Young, 1963; Pessagno, 1967, 1969; Bukry, 1969; Cloud, 1975; Scholle and Cloud, 1977; Dravis, 1979). The Austin Chalk crops out locally from Red River County in northeast Texas, southwest through Dallas, Waco, Austin, San Antonio, Uvalde, and Del Rio, to Val Verde County

[1]Manuscript received, June 7, 1985; accepted, September 4, 1986.

[2]Center for Tectonophysics, Texas A&M University, College Station, Texas 77843. Present address: Department of Earth and Space Sciences, University of California at Los Angeles, Los Angeles, California 90024.

[3]Center for Tectonophysics, Texas A&M University, College Station, Texas 77843.

We thank Clayton W. Williams, Jr., and his company for providing funding for this research and access to well data. We also thank Roy Nurmi of Schlumberger-Doll Research who provided the SEM photomicrographs. Cores were provided by Emily Stoudt, Getty Oil Research; Lyle Baie, Cities Service Research; Rod L. Boane, Exxon Company, U.S.A.; Ronald Nelson, Amoco Production Research; and George Donaldson, University of Texas Bureau of Economic Geology. The assistance of Jody Stevens in the field is gratefully acknowledged. Finally, we thank Peter Bird, Gerhard Oertel, and two anonymous AAPG reviewers for helpful comments on earlier drafts of this manuscript.

[4]Trademark Schlumberger Limited.

in southwest Texas (Figure 1). From Val Verde County, the outcrop extends into northern Mexico, where the lithostratigraphic equivalent is the San Felipe Formation (Dravis, 1979). In general, both the surface and subsurface trends parallel the form of the Gulf Coast geosyncline. Exposures are generally poor, the best existing in quarries, roadcuts, and stream beds. Nowhere along the trend is the complete stratigraphic section exposed, and seldom is more than 30 m of stratigraphic thickness present at any one locality.

The Austin Chalk is best characterized as a very fine-grained carbonate mud containing coarser skeletal tests and fragments, primarily consisting of coccoliths, planktonic and benthonic foraminifera, calcispheres, mollusks, echinoids, and bryozoans. The grain size of the chalk is bimodal, with 75-85% ranging from 0.5 to 4.0 μm, composed primarily of coccolith debris and clay. The remainder is 10-100 μm or larger and consists of coarse carbonate skeletal material. In outcrop, the Austin Chalk has porosities ranging from 30% at Dallas, decreasing southwest along the trend to 9% at Langtry (Cloud, 1975). Subsurface porosity is further reduced, ranging from less than 5 to 16% (Dravis, 1979). We analyzed five representative outcrop samples and four subsurface samples of the Austin Chalk by quantitative x-ray diffraction to ascertain the bulk mineralogy of the chalk and facies related mineralogic trends (Table 1). The average calcite content is 88% for outcrop samples and 83% for subsurface samples. Principal noncarbonate mineral constituents are clay minerals and quartz, with a minor amount of feldspar present in all subsurface samples.

The Austin Chalk is Upper Cretaceous, ranging from the base of the Coniacian Stage to the top of the Santonian Stage (Pessagno, 1967, 1969; Bukry, 1969). The stratigraphy of the Austin Chalk has been comprehensively studied by Durham (1957). However, Pessagno (1969) noted that only one of Durham's units, the Dessau Chalk Member, had been described formally. In this study, the formal and informal stratigraphy presented by Pessagno (1969) for southwest Texas will be used. Lithostratigraphic correlation by us between Pessagno's units for southwest and northeast Texas and Durham's units for the Austin area is presented in Figure 2.

The structural setting of the Austin Chalk has been determined by the Gulf Coast geosyncline, and affected by the Balcones, Luling, Mexia, and Talco fault zones. Faulting throughout the Austin Chalk trend is characterized by en echelon normal faults. The Balcones fault zone is a conjugate normal fault system whose trend closely approximates that of the Paleozoic Ouachita fold and thrust belt from Kinney County in southwest Texas to Dallas County in northeast Texas (Weeks, 1945). The Austin Chalk outcrop trend coincides with the Balcones fault zone.

The Luling, Mexia, and Talco fault zones also parallel the structural grain of the Ouachita fold and thrust belt downdip from the Balcones fault zone. Faults of the Luling, Mexia, and Talco systems generally produce horst-and-graben structures with conjugate normal faults dipping to the southeast and northwest.

Original movement in all of these fault zones may have begun as early as Late Cretaceous. However, all large subsurface faults in Cretaceous strata have equivalent displacements in overlying outcropping Eocene strata. Major movement occurred along all fault zones during the late Oligocene or early Miocene (Weeks, 1945). No evidence indicating a difference in age between the fault zones exists; thus, they are assumed to be contemporaneous.

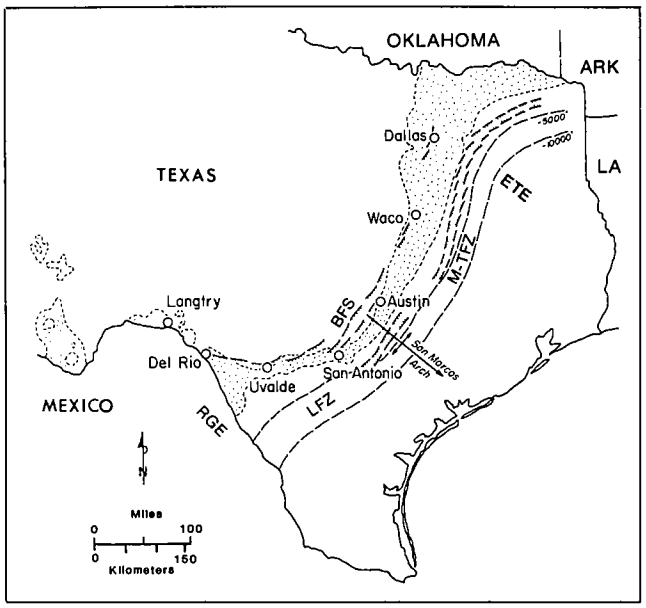

Figure 1—Location map of Texas showing Austin Chalk outcrop trend (shaded), sample locations (open circles), Balcones fault system (BFS), Luling fault zone (LFZ), Mexia-Talco fault zone (M-TFZ), East Texas embayment (ETE), Rio Grande embayment (RGE), and subsurface structure contours on top of Austin Chalk. C.I. = 5,000 ft.

MECHANICAL STRATIGRAPHY

Outcrop Studies

The mechanical stratigraphy of the Austin Chalk was established on the basis of relative fracture intensity (Table 2). Fracture intensity is defined as the average number of fractures intersected per linear meter. A high fracture intensity represents a more brittle response, and a low fracture intensity represents a more ductile response.

The field sampling procedure required three mutually perpendicular linear traverses, two parallel to bedding and the third perpendicular to bedding at each station. As a consequence of the preponderance of subvertical to vertical extension fractures encountered at all localities, the fracture intensity used for comparison is the average of the bedding-parallel traverses. Priest and Hudson (1976) described the sampling technique in detail. Fracture orientation changes systematically with the change in orientation of the Balcones fault zone. At all localities, an orthogonal set of extension fractures is developed. One group of fractures parallels the strike of the Balcones fault zone, and the second group is perpendicular to the first. Each direction is developed in approximately equal abundance.

We measured 2,219 fractures (49 shear fractures) in the Austin Chalk, 1,671 in the Atco Chalk Member, 209 in the

Table 1. Quantitative X-Ray Diffraction Compositional Analysis*

Sample	Q	F	C	D	FD	G	P	K	Ch	I	S/I	S	Stratigraphic Member
Dallas	3	tr	89				tr	2	1	3		2	Atco Chalk
Langtry	4	tr	91	tr		tr	tr	1		2	2		Atco Chalk
Uvalde	5	tr	90				tr	5		tr			Big House Chalk
Del Rio	4	tr	87		tr		tr	1	2	2		4	Dessau Chalk
San Antonio	6	tr	85		tr			5	1	tr		3	Atco Chalk
J. M. Moore (2,675 m)	5	2	85		2			2	2	2			Lower massive chalk
G. Longenbough (2,126 m)	11	2	71				tr	3	4	5		4	Lower massive chalk
Chinn and Asbey (1,878 m)	3	2	89		tr		tr	1	2	2	1		Middle chalk-marl
Ivy B (2,559 m)	12	2	84		2		tr	tr		tr			Middle chalk-marl

*In percentage by volume. Q = quartz, F = feldspar, C = calcite, D = dolomite, FD = ferrodolomite, G = gypsum, P = pyrite, K = kaolinite, Ch = chlorite, I = illite, S/I = smectite/illite, S = smectite, and tr = trace. First five samples are from outcrops; last four samples are from wells.

Dessau Chalk and Burditt Marl Members, and 339 in the Big House Chalk Member. Fracture intensity for the entire Atco Chalk Member outcrop trend ranges from 1.31 to 10.57 fractures/m. The maximum value is from San Antonio and the minimum value is from Lozier Canyon. We obtained a mean of 5.80 fractures/m with a standard deviation of 2.42 fractures/m for the Atco Chalk Member. For the Dessau Chalk and Burditt Marl Members, fracture intensity ranges from 0.86 fractures/m at the Tesquesquite Creek locality in Del Rio to 5.42 fractures/m at Little Walnut Creek in Austin. The mean value of fracture intensity for this middle ductile unit was 2.60 fractures/m with a standard deviation of 1.74 fractures/m. For the Big House Chalk Member, fracture intensity ranges from 1.84 to 8.95 fractures/m, with a mean of 6.33 fractures/m and a standard deviation of 3.27 fractures/m. All traverses for the Big House Chalk Member are from the roadcut adjacent to the Nueces River near Uvalde.

On the basis of fracture intensity, the following mechanical stratigraphy is established: a massive, brittle, lower chalk corresponds to the Atco Chalk Member; a ductile chalk-marl corresponds to the Dessau Chalk and Burditt Marl Members; and a massive, brittle, upper chalk corresponds to the Big House Chalk Member (Figure 3).

We use the term massive to indicate that the upper and lower mechanical-stratigraphic units essentially behave as single homogenous bodies, and that individual beds do not behave independently. Generally, this holds true as long as the intervening marl beds separating the chalk beds are less than or equal to one-tenth the thickness of surrounding chalk beds. This condition applies for the outcrop south of Waco to Lozier Canyon. However, in the Dallas to Waco portion of the outcrop trend, intervening marl beds exceed this thickness ratio, and as a result, fractures tend to terminate within individual chalk beds (Figure 4). Where a significant number of fractures terminate in individual beds, the entire unit cannot be regarded as massive, so each bed is considered as an independent mechanical unit. Although individual beds in this case behave independently, the large-scale mechanical stratigraphy still prevails with fracture intensity in the Atco Chalk Member and Big House Chalk Member usually at least twice that of the Dessau Chalk Member and Burditt Marl Member.

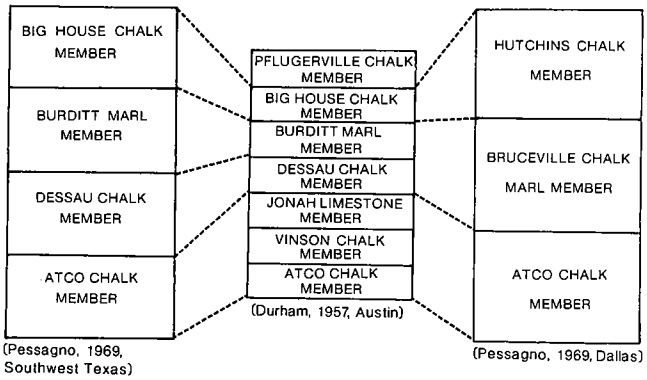

Figure 2—Lithostratigraphic correlation of Austin Chalk. Outcrop localities are cited in references shown with each area.

Fracture intensities exhibit several other significant trends. Among these is a systematic change along the outcrop that can be correlated with the intensity of faulting in the Balcones fault zone. Fracture intensity for the entire trend is greatest in San Antonio (10.56 fractures/m, Table 2). Geologic maps from the *Geologic Atlas of Texas* (Barnes, various dates) indicate that the highest areal density of faulting in the Balcones fault zone occurs in the San Antonio area. Also, the highest fracture intensities occur where the stratigraphic section thins across the San Marcos arch. The juxtaposition of high fracture intensity and high fault density may be related to thinning of the Cretaceous strata across this regional upwarp.

The other predominant trend in fracture intensity is associated with structural position. At a given sample locality, grabens always possess a higher fracture intensity than intervening horsts. The increased fracture intensity in the grabens may be ascribed to two sources. First, faults of the Balcones system are highly dilatant as is the graben itself, resulting in an increased fracture intensity. Second, and more important, fractures striking normal to faults of the Balcones system are much better developed in the grabens. The dilatant nature of the fault zones and origin of the cross-trending fractures and associated faults are discussed in Corbett (1982).

Core and Log Analyses

We analyzed oriented cores from 8 wells and 22 FILs to determine the mechanical stratigraphy of the Austin Chalk

Table 2. Outcrop Fracture Intensity Data

Locality and Stratigraphic Member	Average Fracture Intensity (fracture/m)*	Bed Thickness (cm)	Fracture Intensity (fractures/m)	Number of Fractures/ Traverse Length (m)	Structural Position
		45.7	2.66	17/6.40	Graben
Dallas (D)	X = 4.72	50.8	7.27	72/9.91	Graben
Atco Chalk	S = 1.97	121.9	5.01	84/16.76	Graben
		137.2	3.94	30/7.62	Graben
		30.0	6.56	92/14.02	Graben
Waco (W)	X = 5.35	40.6	3.77	50/13.26	Graben
Atco Chalk	S = 1.44	66.0	5.73	55/9.66	Horst
Austin (A)	X = 3.80	304.8	2.17	53/24.39	Graben
Dessau Chalk	S = 1.62	50.8	5.42	62/11.43	Graben
		35.6	8.49	44/5.18	Graben
		45.7	10.57	29/2.74	Graben
		50.8	6.95	36/5.18	Graben
		55.9	6.89	21/3.05	Graben
		71.1	6.22	74/11.89	Horst
San Antonio (SA)	X = 7.12	96.5	6.56	71/10.82	Graben
Atco Chalk	S = 2.07	106.7	9.37	50/5.34	Graben
		121.9	5.60	29/5.18	Horst
		129.5	6.10	158/25.91	Graben
		243.8	2.99	31/10.37	Horst
		365.8	8.42	190/22.56	Graben
		30.5	8.55	133/15.54	Graben
Uvalde (U)	X = 6.33	40.6	5.99	73/12.19	Horst
Big House Chalk	S = 3.28	106.7	1.84	28/15.24	Horst
		109.2	8.95	105/11.73	Graben
Del Rio (DRT)		45.7	1.64	25/15.24	Horst
Dessau Chalk and	X = 1.80	45.7	2.89	44/15.24	Graben
Burditt Marl	S = 1.02	91.4	0.86	25/29.00	Horst
		30.5	6.19	99/16.01	Graben
Langtry (LA)	X = 4.72	66.0	7.17	94/13.11	Graben
Atco Chalk	S = 2.39	68.6	3.41	77/22.56	Graben
		86.4	2.08	63/30.34	Graben
		10.2	9.73	86/8.84	Anticline
Lozier Canyon (LC)	X = 4.72	20.3	4.46	66/15.24	Anticline
Atco Chalk	S = 3.61	81.3	3.33	31/9.30	Anticline
		96.5	1.31	20/15.24	Anticline

*X = locality mean fracture intensity; S = standard deviation.

in the subsurface (Table 3). No well cored the entire chalk interval; however, in composite the cores transect the entire interval. Fracture intensity is highest in the upper and lower third of the chalk; thus, the subsurface mechanical stratigraphy is analogous to the outcrop trend.

In addition to our observations, the fracture data presented here are synthesized from reports by Core Laboratories Inc., Houston, Texas, for the Getty wells, and from a Cities Service Company in-house report for its Brown-Dunlap A-1 core. Fracture intensities range from less than 0.10 fractures/m for the Chinn and Asbey 3 wells to 10.56 fractures/m for the Brown-Dunlap A-1 well. All cores from the Atco Chalk Member and Big House Chalk Member exhibit an orthogonal set of extension fractures, one group parallel to the strike of bedding, the other parallel to the bedding dip direction. Fractures encountered in the cores overwhelmingly have dips approaching vertical, are usually completely filled with sparry calcite cement, and generally occur in swarm. Fracture widths range from 0.01 to 1.0 mm.

We interpreted 22 FIL in Lee and Burleson Counties to determine the mechanical stratigraphy and fracture orientations in the Giddings field and surrounding area. A FIL is a presentation format for the microresistivity measurements made by the four-arm dipmeter. Babcock (1978) and Brown (1978) presented thorough discussions on using the dipmeter to interpret natural fractures in boreholes.

Five wells yielded no fracture information due to mechanical malfunctions or apparent lack of fracturing in the formation. The remaining 17 wells indicate qualitatively that the mechanical stratigraphy identified in outcrop and confirmed in core analysis for the subsurface is reflected in the FIL data (Table 3). For example, the num-

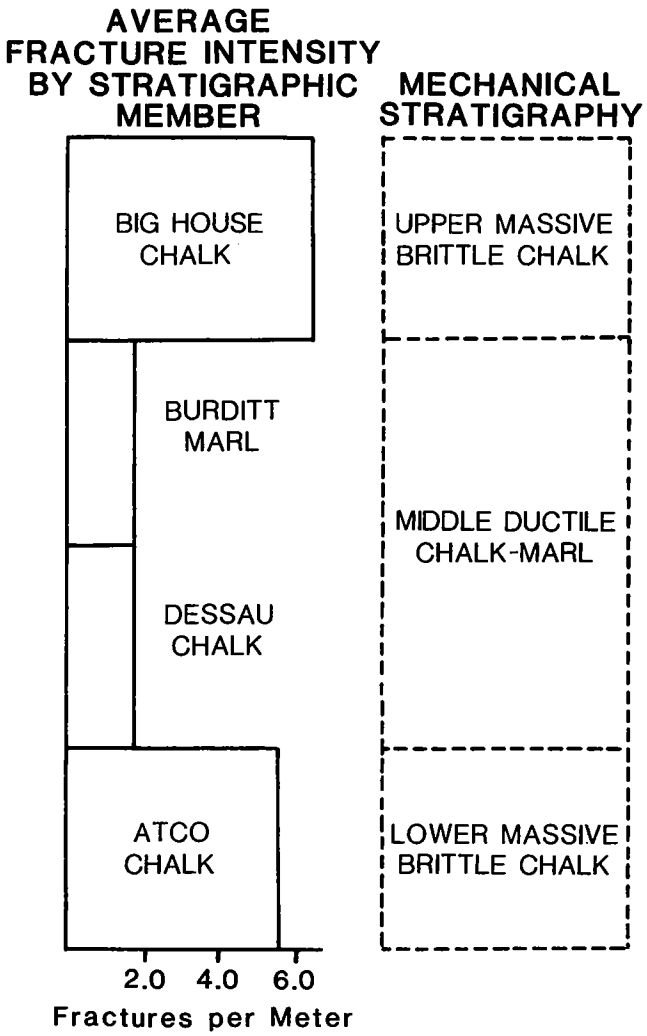

Figure 3—Average fracture intensity (in fractures/meter), by stratigraphic member, for Austin Chalk and mechanical stratigraphy determined by this criteria.

ber of washouts and breakouts is minimal in the ductile Dessau Chalk and Burditt Marl Members.

EXPERIMENTAL ROCK DEFORMATION

We conducted rock deformation experiments to determine: (1) if the mechanical stratigraphy established from field and subsurface studies is reflected in the relative strengths and ductilities of representative samples deformed in the laboratory; (2) if lateral facies variations such as texture and diagenesis are related to the strength and ductility of the Atco Chalk Member; and (3) which physical parameters most directly influence the strength and ductility characteristics of the chalk. Laboratory analysis can lead to an understanding of the causative factors that determine mechanical response and thus provide a basis for extrapolation and prediction of where natural fracturing occurs.

All samples were right circular cylinders 5.1 cm in diameter and 10.2 cm long. We ground the ends with an 80 grit

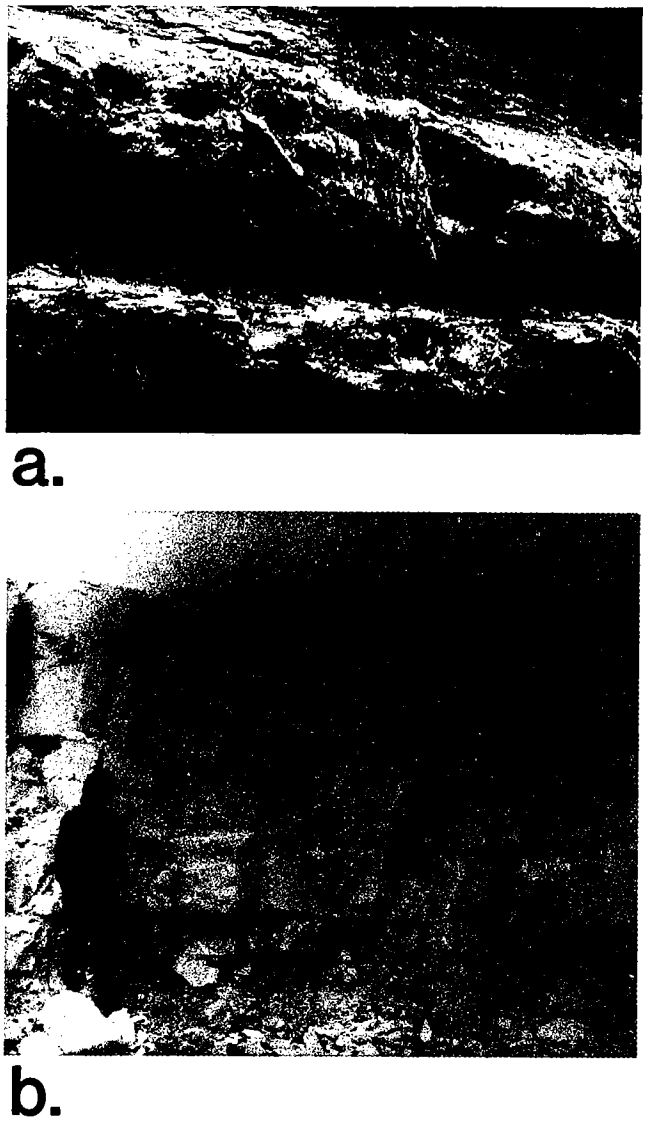

Figure 4—Representative fracture styles in Austin Chalk outcrop trend. (a) Fractures terminating in individual chalk bed at interface with surrounding marl beds (hammer is 32 cm long for scale); middle ductile chalk-marl, Cameron Park, Waco, Texas. (b) Fractures cutting several massive chalk beds (individual is 1.88 m tall for scale); upper massive brittle chalk, San Antonio Portland Cement Quarry, San Antonio, Texas.

wheel to 0.001 cm of parallel, and shortened 20 samples dry, at confining pressures ranging from 10 to 70 MPa, at 24°C, and at a constant displacement rate of 2.5×10^{-4} sec^{-1} (Table 4). Our confining pressures were chosen to simulate a range of burial depths and ambient effective confining pressures comparable to present-day hydrocarbon exploration in the Austin Chalk subsurface trend. We used 0.23 bars/m of overburden, assuming an average density of 2.65 g/cm^3, and a pore pressure of 0.11 bars/m of burial, assuming normal pore pressure equals 0.43 of overburden pressure, to establish the confining pressures representative of the depth range from 833 to 5,833 m. We also assumed that the law of effective pressure applied to the Austin Chalk, so the con-

Table 3. Subsurface Fracture Intensity from Cores and Fracture Identification Logs

Borehole/County in Texas	Fracture Intensity (fractures/m)	Fracture Style	Stratigraphic Member
G. Longenbough 1/Leon	0.55	Shear fractures and small faults	Atco Chalk
J. M. Moore 1/Trinity	1.84	Extension fractures	Atco Chalk
Chinn and Asbey 3/Zavalla	<0.10	1 shear fracture and 1 extension fracture	Dessau Chalk–Burditt Marl
Ivy B 1/Fayette	0.98	Extension and shear fractures	Dessau Chalk–Burditt Marl
Brown Dunlap A-1/Brazos	10.50	Extension fractures	Atco Chalk
W. E. Beall 1/Frio*	0.50	Extension fractures	Big House Chalk
William Nash 1/Brazos	4.64	Extension fractures	Atco Chalk
Margrave 1/ Brazos	4.57	Extension fractures	Big House Chalk

Borehole/County in Texas	Number of Washouts and Breakouts**	Stratigraphic Member
1 Miertschin/Lee	1	Big House Chalk
	3	Atco Chalk
Noack-Mitschke/Lee	3	Atco Chalk
Elford Bigon/Lee	2	Atco Chalk
	1	Dessau Chalk–Burditt Marl
E. J. Parrish 3/Lee	4	Atco Chalk
Lou Ella Cheeks 1/Lee	4	Atco Chalk
Schmidt Massey 1/Lee	1	Dessau Chalk–Burditt Marl
	2	Atco Chalk
Jas Hunt A-166/Lee	2	Atco Chalk
E. J. Parrish 1-A/Lee	1	Big House Chalk
	1	Dessau Chalk–Burditt Marl
Don Bisset 1/Lee	1	Atco Chalk
M. Whitewell 1/Lee	7	Atco Chalk
Mamie Schmidt 3/Lee	5	Atco Chalk
Schmidt 2/Lee	5	Atco Chalk
Humphrey-Benson 1/Lee	3	Big House Chalk
Benn 1/Burleson	4	Big House Chalk
Leo Haverman 1/Burleson	1	Dessau Chalk–Burditt Marl
Gaas 1/Burleson	1	Atco Chalk
Rust 1/Burleson	4	Atco Chalk

*Core in a poorly preserved condition for determination of fracture intensity.
**Washout and breakout zones are thought to correlate with highly fractured zones.

fining pressure of dry tests (P_c) can be equated to the effective pressure ($P_e = P_c - P_{pore\ fluid}$) at a given depth (Handin et al, 1963).

We selected a strain rate of 2.5×10^{-4} sec^{-1} to allow a sufficient number of tests to be performed to assess the relationship of intrinsic rock properties to strength and ductility. This rate is sufficiently slow for the operative mechanisms of deformation to be similar to those in nature.

Inspection of the experimental stress-strain curves (Figure 5; Table 4) indicates the following:

1. At all confining pressures, the specimens from Dallas (D) and San Antonio (SA) are the weakest and most ductile.
2. Ductility of specimens from Langtry (LA), Uvalde (U), and Del Rio (DRT) increases with increasing confining pressure, as expected.
3. At confining pressures of 17, 34, and 70 MPa, the specimens from Del Rio are intermediate in strength between those from Dallas and San Antonio, and those from Langtry and Uvalde.
4. The samples from Langtry and Uvalde are remarkably strong.
5. Although the mechanical behavior of the Dallas and San Antonio chalks are similar, the yield strengths of the San Antonio specimens are consistently lower than those for the Dallas specimens at a given confining pressure.

The Langtry, Del Rio, and Uvalde samples are representative of the lower massive chalk (Atco Chalk Member), the middle chalk-marl (Dessau Chalk–Burditt Marl Members), and the upper massive chalk (Big House Chalk Member), respectively. The San Antonio and Dallas samples are representative of the lower massive chalk (Atco Chalk Member). The disparity in strength between Dallas, San Antonio, and Langtry samples, all from the same mechanical-stratigraphic unit, is related to differences in physical properties such as composition and porosity.

STATISTICAL ANALYSIS OF EXPERIMENTAL DATA

Multiple linear regression is a technique whereby the relationship between a dependent variable, in this study rock

Table 4. Experimental Rock Deformation Data*

Sample	Confining Pressure (MPa)	Fracture Strength (MPa)	Ultimate Strength (MPa)	Strain at Ultimate Strength (%)	Remarks
D-5	10	52	52	1.35	Single shear fracture
SA-4	10	42	42	1.99	Single shear fracture
DRT-1	10	138	138	0.92	Conjugate shear fractures
D-4	17	—	59	2.26	Luders' bands barreled
SA-1	17	—	52	6.00	Luders' bands barreled
DRT-2	17	153	153	1.13	Single shear fracture
LA-1	17	218	218	1.00	Single shear fracture
U-2	17	259	259	1.29	Very brittle conjugate shear fractures and extension fracture
U-4	17	262	262	1.27	Very brittle conjugate shear fractures and extension fracture
D-1	34	—	64	8.59	Slightly barreled
SA-3	34	—	72	6.88	Slightly barreled
DRT-4	34	168	168	2.29	Conjugate shear fractures
U-3	34	260	260	2.31	Single shear fracture
LA-3	34	265	265	1.88	2 parallel shear fractures
LA-2	34	272	272	2.07	2 parallel shear fractures
D-2	70	—	84	8.99	Uniform shortening
SA-5	70	—	106	8.93	Uniform shortening
DRT-3	70	—	228	8.40	Luders' bands barreled
LA-5	70	—	302	4.21	Luders' bands barreled
U-1	70	319	319	4.74	Single shear fracture

*Fracture strength = differential stress supported at failure; ultimate strength = fracture strength for failed specimens; D = Dallas; SA = San Antonio; DRT = Del Rio; LA = Langtry; U = Uvalde; and — = specimen did not fracture during the experiment.

strength, and numerous independent variables such as porosity, mineralogic composition, strain, and confining pressure may be investigated simultaneously. Details of the technique are in Younger (1979). The fundamental objectives of regression modeling are to investigate the degree to which the independent variables describe the variation of the dependent variable, and to provide a predictive tool for estimating the dependent variable, given new values of the independent variables.

The data matrix (Table 5) consists of 20 observations and 7 variables. The dependent variable (strength) for each observation is either the fracture strength or the strength at the strain equivalent to failed specimens for ductile specimens at a given confining pressure. For example, at 70 MPa confining pressure, specimens U-1 and LA-5 failed at 4.74 and 4.21% strain, respectively. We determined the strength of specimens D-2, SA-5, and DRT-3 by inspecting the stress-strain curves (Figure 5d) at 4.50% strain for these ductile responses. We determined porosity for each bulk sample using a helium porosimeter in the Petroleum Engineering Laboratory at Texas A&M University. Mineralogy for each bulk sample is from quantitative x-ray diffraction analysis (Table 1). Confining pressure (P_c) is fixed for each experiment, and strain is that at failure or an equivalent value for ductile responses.

In Table 5, the values of porosity, calcite, smectite, and total clay are constant for a given geographic locality. These values represent those determined for the entire bulk sample (25 kg) from a given locality. Porosity values are the average of four samples, 2 parallel to bedding and 2 perpendicular, for each bulk sample. We determined composition from powdered sample splits for each bulk sample. Porosity varied no more than 3% for a given bulk sample, and our porosity values compare well with those determined in previous studies (Cloud, 1975; Dravis, 1979) for the geographic areas represented. The variation of composition in any given bulk sample is unknown, but we expect that it is of the same order as the variation in porosity because changes in porosity are strongly correlated with accompanying changes in bulk mineralogy. Additionally, we do not want to imply that the porosity and composition values determined for any bulk sample are strictly representative of all possible values for a specific geographic area. However, we believe the values are representative of the areas from which they were collected and reflect the average properties of that area. For the purpose of our model, which is to determine the effect of intrinsic rock properties on the mechanical behavior of experimentally deformed samples of the Austin Chalk, the variation within a given lithostratigraphic unit or geographic locality is irrelevant, as long as there is no significant variation within a given bulk sample used in the experiments. The model may be used to predict the variation in strength in a geographic area or lithostratigraphic unit for different samples, if the intrinsic properties of composition and porosity are known.

Initially, we tested the model:

$$\text{Strength} = \alpha + \delta_1\,\text{porosity\%} + \delta_2\,\text{calcite\%} + \delta_3\,\text{smectite\%} + \delta_4\,\text{total clay\%} + \delta_5\,P_c + \delta_6\,\text{strain\%} + \epsilon. \quad (1)$$

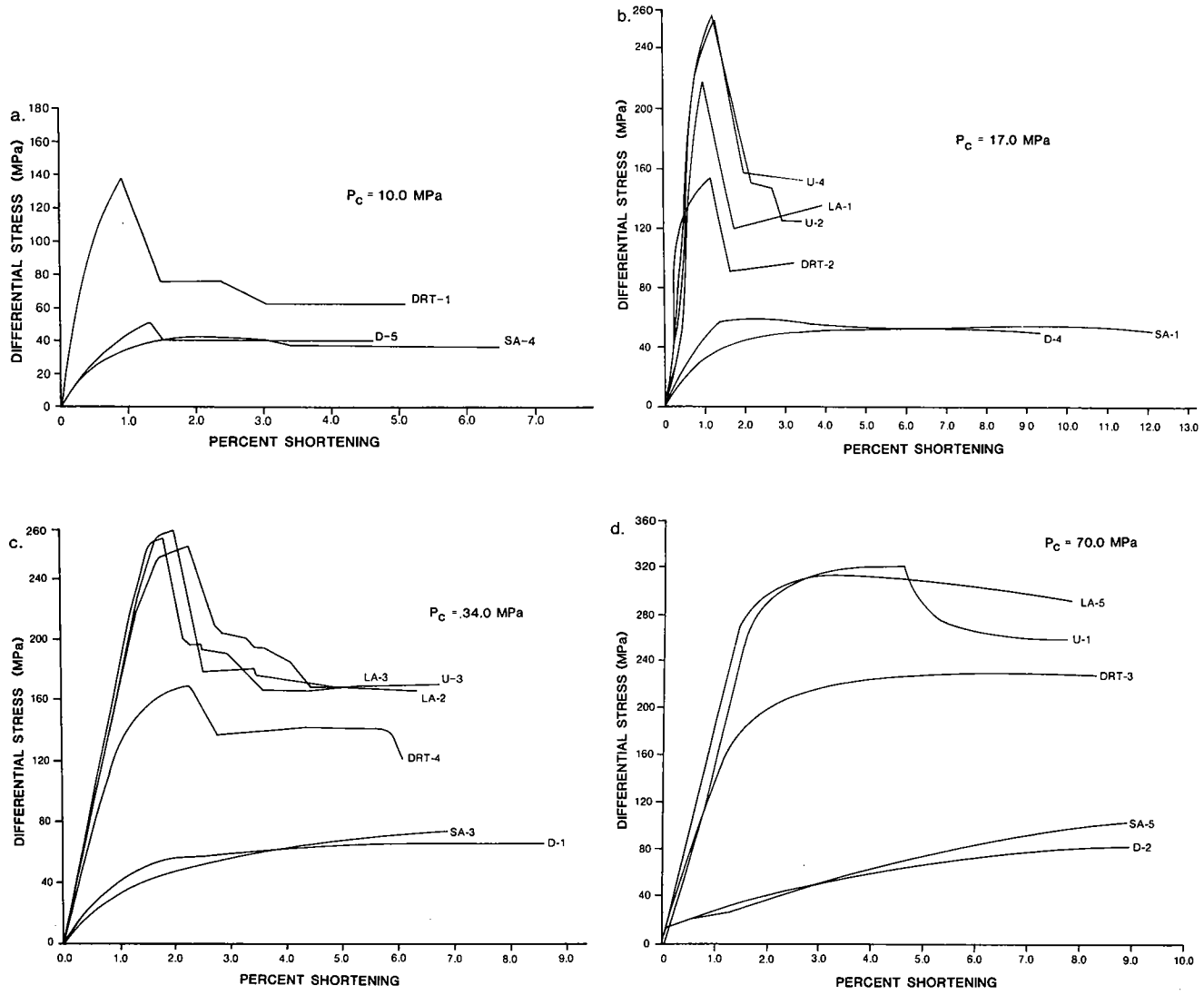

Figure 5—Stress-shortening curves for experimentally deformed specimens of Austin Chalk, at confining pressures of: (a) P_c = 10.0 MPa, (b) P_c = 17.0 MPa, (c) P_c = 34.0 MPa, and (d) P_c = 70.0 MPa. Sample numbers refer to localities discussed in text: D = Dallas, SA = San Antonio, U = Uvalde, DRT = Del Rio Tesquesquite Creek, and LA = Langtry.

The R^2 net correlation coefficient for this model equals 0.986. Essentially, this coefficient indicates that 98.6% of the variation in strength may be described by the independent variables. The F-test for the significance of the regression equation indicates that at a 99.9% confidence level the regression is significant. Hypothesis tests reveal that there is strong internal correlation among the independent variables, e.g., percent smectite with percent total clay.

We used several variable selection techniques to reduce the internal correlations and provide a model that describes the process with as few independent variables as possible. Variable selection techniques are not truly statistical methods, but are mathematical methods whereby the experimenter may decide, on a subjective basis, which variables to retain in a model and which to reject. We used the following criteria to decide whether to retain or reject a variable and to arrive at a final model:

1. Variables that were retained should possess the lowest possible internal correlations.
2. The final model should consist of as few independent variables as possible without significantly reducing the R^2 net correlation coefficient or the confidence level (both must be greater than 95.0%).
3. The final model should contain the variables that possess the strongest simple correlation with rock strength.
4. If two variables were colinear and one contained the information of the other, e.g., percent total clay and percent smectite, the simple variable was retained and the composite variable rejected.

Using the variable selection techniques, we chose the following model:

$$\text{Strength} = \alpha + \delta_1 \,\text{porosity\%} + \delta_2 \,\text{smectite\%} + \delta_3 \,\text{strain\%} + \epsilon. \quad (2)$$

Table 5. Data Matrix for Multiple Linear Regression Analysis

Strength	Porosity (%)	Calcite (%)	Smectite (%)	Total Clay (%)	P_c (MPa)	Strain (%)	Specimen No.*
51.99	26.95	89.0	2.0	8.0	10.0	1.35	D-5
45.00	26.95	89.0	2.0	8.0	17.0	0.96	D-4
51.00	26.95	89.0	2.0	8.0	34.0	2.30	D-1
65.00	26.95	89.0	2.0	8.0	70.0	4.50	D-2
42.05	27.17	85.0	3.0	9.0	10.0	1.99	SA-4
35.61	27.17	85.0	3.0	9.0	17.0	1.03	SA-1
48.42	27.17	85.0	3.0	9.0	34.0	2.29	SA-3
67.00	27.17	85.0	3.0	9.0	70.0	4.50	SA-5
261.96	13.37	90.0	0.0	5.0	17.0	1.27	U-4
258.68	13.37	90.0	0.0	5.0	17.0	1.29	U-2
260.01	13.37	90.0	0.0	5.0	34.0	2.31	U-3
318.91	13.37	90.0	0.0	5.0	70.0	4.74	U-1
137.56	8.90	87.0	4.0	9.0	10.0	0.92	DRT-1
153.25	8.90	87.0	4.0	9.0	17.0	1.13	DRT-2
168.04	8.90	87.0	4.0	9.0	34.0	2.29	DRT-4
224.00	8.90	87.0	4.0	9.0	70.0	4.50	DRT-3
218.04	11.19	91.0	1.0	5.0	17.0	1.00	LA-1
265.47	11.19	91.0	1.0	5.0	34.0	1.88	LA-3
272.36	11.19	91.0	1.0	5.0	34.0	2.07	LA-2
301.83	11.19	91.0	1.0	5.0	70.0	4.21	LA-5

*Listed for reader's convenience; not part of data matrix.

The R^2 net correlation coefficient for model 2 is 0.978. Model 2 results in the lowest internal correlations and the lowest number of independent variables, and it represents a loss of less than 1% of the value of R^2 compared to model 1 with six independent variables. Furthermore, model 2 is significant at a 99.9% confidence level, all three predictor variables have confidence levels of 99.9%, and internal correlations have a high probability of occurring by chance. Thus, for this study, we selected model 2 as the regression equation representative of the variation of strength with intrinsic rock properties for the Austin Chalk.

DISCUSSION OF RESULTS

Statistical Analysis

It may be argued that 20 experiments, performed on samples from 5 geographic localities, are insufficient to adequately constrain the control exerted by composition and porosity on the strength of the Austin Chalk. However, the strength of regression model 2, expressed by the robust correlation coefficient and very high confidence levels, suggests that the sampling density and number of experiments adequately describe the process. Undoubtedly, a greater areal diversity of samples and number of observations would further constrain the model but would not significantly improve it.

Of interest is the degree to which each of the independent variables affects strength. Using model 2, we found that porosity alone can account for 68.9% of the strength variation. By adding smectite content, 93.3% of the variation in strength can be accounted for, and with strain included, the model accounts for 97.8% of the strength variation. Although strain at failure is a result in the experimental studies, in natural geologic deformation it is an independent variable and can be correlated with confining pressure.

That smectite content (given porosity) accounts for nearly 25.0% of the variability in strength is of special interest. We included percent smectite in the initial and final regression models and excluded other individual clay minerals, based on the established anomalously low strength and friction of smectite clays. The effects of smectite clays in simulated gouges have been studied by Summers and Byerlee (1977), Logan et al (1981), and Shimamoto and Logan (1981). They found that the tangent coefficient of friction for Wyoming bentonite (Na-montmorillonite) and Arizona bentonite (Ca-montmorillonite) at 100 MPa confining pressure is low (0.22), and that smectite in quantities as low as 5% (by volume) controls the sliding mode, having the effect of producing stable sliding as opposed to stick-slip. In contrast, in the natural fault gouge recovered from the U.S. Geological Survey Dry Lake Valley well along the San Andreas fault zone, the smectite content does not control the strength of the gouge (Logan et al, 1981). Bird (1984) experimentally investigated the hydration states and frictional properties of pure Na- and Ca-montmorillonites. He reported secant coefficient of friction values as low as 0.27 for Na-montmorillonite, and an average value of 0.34 for Ca-montmorillonite in the top 10 km of strike-slip and normal fault zones. Furthermore, Bird's study tied the abnormally low friction values to the hydration state of the clay. Within the range of confining pressures for experiments on the Austin Chalk (10-70 MPa), the presence of at least one complete adsorbed water layer in the clay structure is predicted by Bird's data, and a correspondingly low coefficient of friction for smectite clays.

In the current analysis, smectite content (given porosity) has a strong negative correlation (25%) with strength for the Austin Chalk. Comparing strength with confining pres-

sure for the low-porosity Uvalde (Big House Chalk Member), Langtry (Atco Chalk Member), and Del Rio (Dessau Chalk–Burditt Marl Members) samples, it is apparent that smectite content exerts a large influence on strength (Figure 6). Generally, the high-porosity samples are stronger, which is the converse of the relationship for all samples. However, the smectite content (4%) is greatest in the lowest porosity (8.9%) Del Rio samples.

To further investigate the relationship of strength and smectite content, we tried regression analysis involving only the low-porosity samples from Del Rio, Langtry, and Uvalde. Although this analysis was unfeasible due to strong internal correlations, several interesting trends are obtained from the correlation matrix:

1. Total clay content has the highest simple correlation with strength and can account for 84% of the variation.
2. Smectite content can account for 83% of the strength variation and is the factor having the second highest simple correlation.
3. Porosity over the limited range of these samples can account for 77% of the variation in strength. All three predictors are significant at a 99.0% confidence level. Apparently, smectite content best predicts strength for samples of low porosity. Noteworthy is that for the limited number of samples, a strongly negative correlation (96.0%) between porosity and smectite content exists at the 99.0% confidence level.

Analysis of Mechanical Behavior

In addition to the influence of porosity, smectite content, and confining pressure on strength, we found strong negative correlations between the coefficient of friction and confining pressure, and between the coefficient of friction and smectite content.

The experimental results, viewed in Mohr diagrams, illustrate that the angle θ between σ_1 and the fracture surfaces increases with confining pressure (Figure 7). The angle of internal friction ϕ systematically decreases ($\theta = 45 - \phi/2$). The implication is that with increasing confining pressure the chalk tends to approach a theoretically frictionless material.

The strong effect of smectite content on the coefficient of friction μ ($\mu = \tan\phi$) is striking (Figure 8). The coefficient of friction decreases exponentially with increasing smectite content. The presence of only 1% smectite apparently is sufficient to decrease the coefficient of friction by at least a factor of two. The presence of 4% smectite further reduces the coefficient of friction, but at a significantly reduced rate. The tangent value of $\mu = 0.18$ for the Del Rio sample at 70 MPa confining pressure is lower than that reported by Shimamoto and Logan (1981) for pure smectite. The ability of 1% smectite to reduce the coefficient of friction by a factor of two underscores the role played by this clay mineral in controlling fracturing of the Austin Chalk.

To investigate the influence of smectite further, we used scanning electron microscopy to delineate the mode of

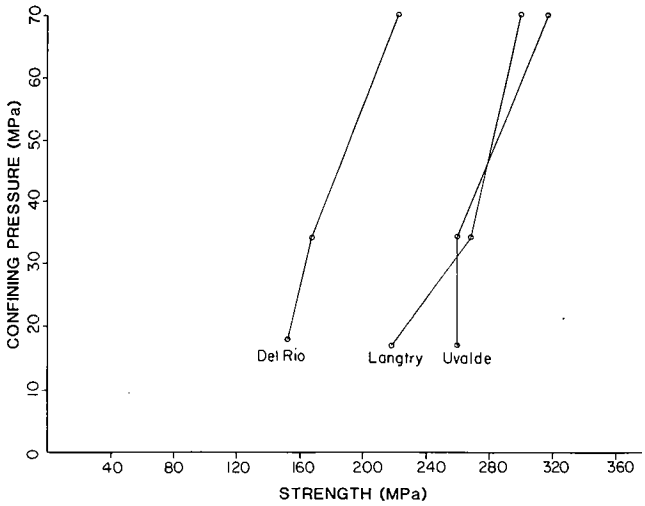

Figure 6—Plot of fracture strength versus confining pressure for experimentally deformed specimens from Del Rio (DRT, 8.90% porosity, 4% smectite), Langtry (LA, 11.10% porosity, 1% smectite), and Uvalde (U, 13.37% porosity, 0% smectite).

smectite occurrence in undeformed and deformed specimens (Figure 9). In undeformed chalk, all clay minerals including smectite occur as discrete, amorphous, aggregate masses ranging from 10 to 30 μm in diameter. This size is significantly larger than the average grain size in the chalk, which is 1.0-4.0 μm. In experimentally deformed specimens, small (0.5 μm) clay mineral fragments are randomly distributed along the fracture surfaces. We believe the large clay masses may have acted as soft inclusions in the chalk. That is, they served as stress concentrators and localized the formation of shear fractures, thus controlling the mode of failure, strength, and strain at failure.

Correlating Experimental Results to Field and Subsurface Conditions

Using multiple linear regression analysis, we found that porosity had the highest correlation with strength. Experimental studies showed that high-porosity chalks, characteristic of the outcrop from Dallas southwest to San Antonio, do not fail by discrete fracture at confining pressures exceeding 10 MPa. This confining pressure corresponds well to reconstructions of maximum depths of burial along this portion of the outcrop trend, assuming normal pore pressure. The role of smectite in determining strength for these high porosities is minimal and is not expected to exert a control on fracturing.

Smectite appears to be the factor most influential on Austin Chalk strength at low porosities characteristic of the outcrop trend from San Antonio west to Langtry, and the subsurface. Absolute laboratory strengths of specimens from Uvalde (Big House Chalk Member), Del Rio (Dessau Chalk–Burditt Marl Members), and Langtry (Atco Chalk Members) are quite high, with differential stresses ranging from 150 to 300 MPa. Stresses of this magnitude are unlikely in the tectonic environment of the Gulf Coast. At

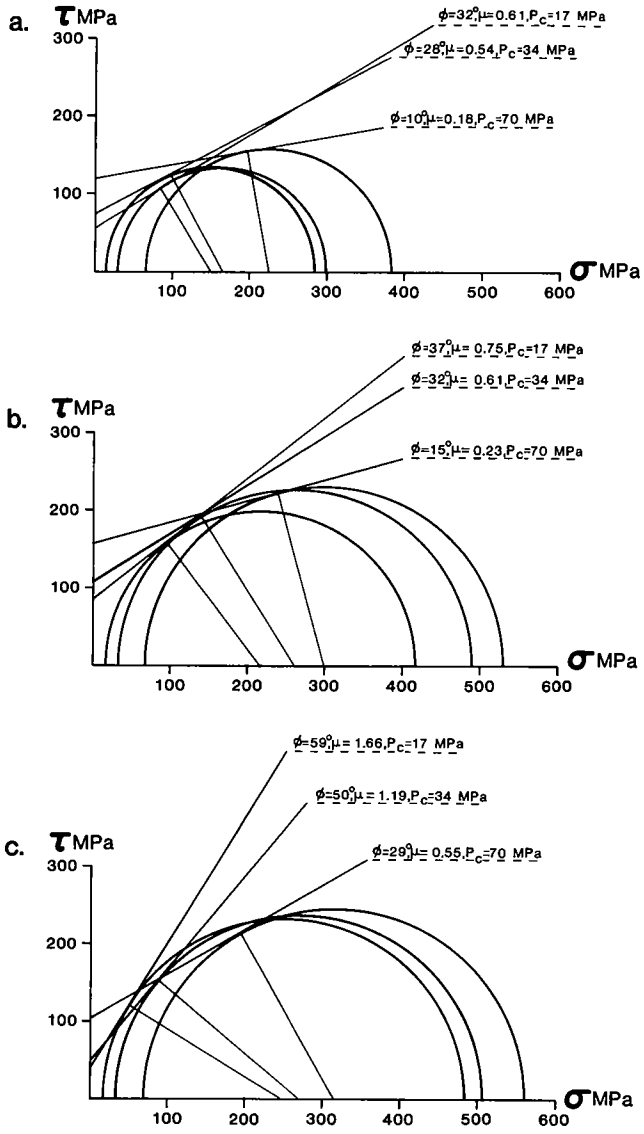

Figure 7—Mohr circle plots for low-porosity, experimentally deformed specimens of Austin Chalk from: (a) Del Rio (DRT, 8.90% porosity, 4% smectite), (b) Langtry (LA, 11.10% porosity, 1% smectite), and (c) Uvalde (U, 13.37% porosity, 0% smectite).

strain rates more representative of natural geologic deformation, lower values of strength probably would be obtained, although the magnitude of this reduced strength is unknown.

CONCLUSIONS

The mechanical stratigraphy of the Austin Chalk defined on the basis of relative outcrop fracture intensity consists of three mechanical units: (1) an upper massive fractured chalk, (2) a middle ductile chalk-marl, and (3) a lower massive fractured chalk. The three mechanical-stratigraphic units correspond to the Big House Chalk Member, the Dessau Chalk and Burditt Marl Members, and the Atco Chalk Member, respectively. In addition, the mechanical stratigraphy of the subsurface trend is analogous to that defined for the outcrop trend.

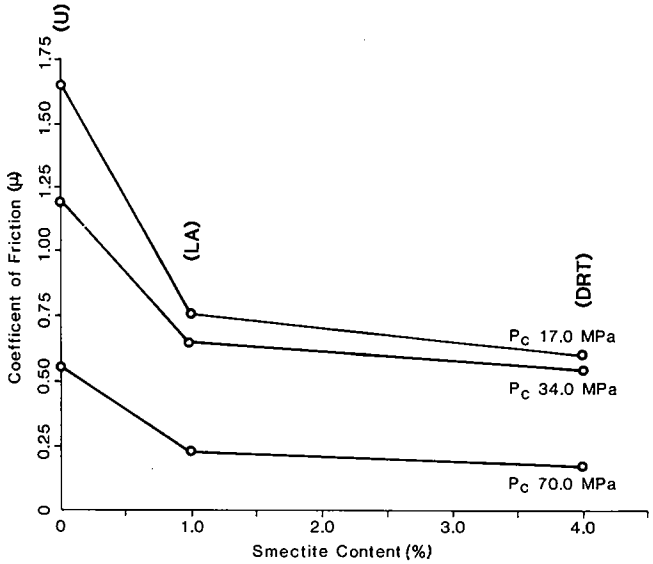

Figure 8—Smectite content versus coefficient of friction for low-porosity, experimentally deformed specimens of Austin Chalk. Localities as in Figure 7.

Fracture intensity along the outcrop trend changes systematically, coincident with the intensity of faulting in the Balcones fault zone. We found the highest average fracture intensity (10.56 fractures/m) in the San Antonio area, where the most abundant faulting in the Balcones system and the stratigraphically thinnest section of Austin Chalk occur.

Experimental rock deformation confirms the mechanical stratigraphy identified in outcrop and subsurface, over a confining pressure range of 10 to 70 MPa for specimens of similar physical properties. The samples from Langtry (Atco Chalk Member) and Uvalde (Big House Chalk Member) are always stronger than those from Del Rio (Dessau Chalk Member).

Multiple linear regression analysis identified three parameters that have the strongest influence on rock strength. Porosity accounts for 68.9% of the variation in strength, smectite content accounts for 24.4% (given porosity), and percent axial strain accounts for 4.7% (given porosity and smectite content).

For low-porosity specimens (Uvalde, Langtry, Del Rio), smectite content appears to have the largest influence on rock strength and can account for 83% of the variation. The presence of 1% smectite is sufficient to reduce the strength by 6% at 70 MPa and 17% at 10 MPa confining pressure, and 4% smectite reduces the strength by 30% to 42% at similar respective confining pressures. The coefficient of friction is reduced by at least a factor of two by the presence of 1% smectite and is further reduced by 4% smectite.

SEM photomicrographs indicate that in undeformed chalk, the clay minerals occur as large (30 μm), discrete, amorphous aggregates randomly distributed throughout the very fine-grained (0.5-4.0 μm) chalk matrix. Small

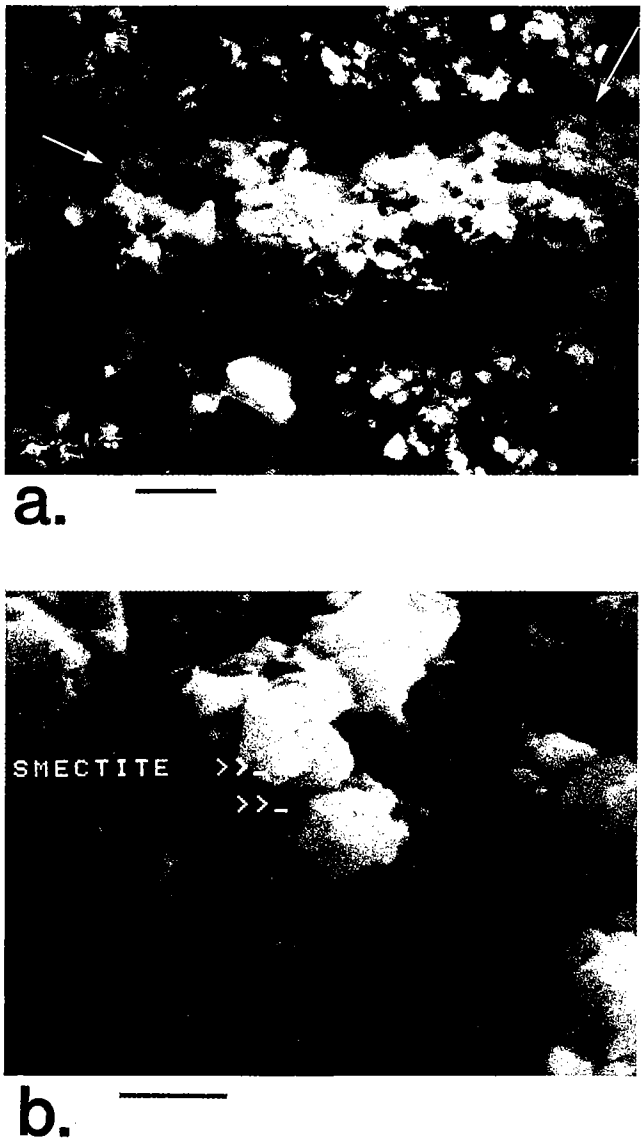

Figure 9—SEM photomicrographs of clay minerals (identified by energy dispersive x-ray analysis) in Austin Chalk. (a) Arrows indicate large, amorphous clay mineral aggregate in finer grained chalk matrix. Dessau chalk (DRT) porosity plug; bar scale = 10 μm. (b) Small smectite clay fragments on shear fracture surface of experimentally deformed sample DRT-2; bar scale = 1 μm.

(≤0.5 μm) clay-mineral fragments are randomly distributed along the experimental shear fracture surfaces. The large clay masses appear to have acted as soft inclusions concentrating the stress and thus localizing shear fractures and controlling failure.

REFERENCES CITED

Babcock, E. A., 1978, Measurement of subsurface fractures from dipmeter logs: AAPG Bulletin, v. 62, p. 1111-1126.

Barnes, V. E., various dates, The geologic atlas of Texas: Austin, University of Texas Bureau of Economic Geology, 38 sheets, scale, 1:250,000.

Bird, P., 1984, Hydration-phase diagrams and friction of montmorillonite under laboratory and geologic conditions, with implications for shale compaction, slope stability, and strength of fault gouge: Tectonophysics, v. 107, p. 235-260.

Brown, R. O., 1978, Application of fracture identification logs in the Cretaceous of north Louisiana and Mississippi: Gulf Coast Association of Geological Societies Transactions, v. 28, p. 75-91.

Bukry, D., 1969, Upper Cretaceous coccoliths from Texas and Europe: University of Kansas Paleontological Contributions, Protista, Article 2, 79 p.

Cloud, K. W., 1975, The diagenesis of the Austin Chalk: Master's thesis, University of Texas at Dallas, Dallas, Texas, 70 p.

Corbett, K. P., 1982, Structural stratigraphy of the Austin Chalk: Master's thesis, Texas A&M University, College Station, Texas, 111 p.

Dravis, J. J., 1979, Sedimentology and diagenesis of the Upper Cretaceous Austin Chalk formation, south Texas and northern Mexico: PhD dissertation, Rice University, Houston, Texas, 513 p.

Durham, C. O., Jr., 1957, The Austin Group in central Texas: PhD dissertation, Columbia University, New York, New York, 130 p.

Handin, J., R. V. Hager, Jr., M. Friedman, and J. N. Feather, 1963, Experimental deformation of sedimentary rocks under confining pressure: pore pressure tests: AAPG Bulletin, v. 47, p. 717-755.

Hill, R. T., 1887, The Texas section of the American Cretaceous: American Journal of Science, v. 34, p. 287-309.

Logan, J. M., N. G. Higgs, and M. Friedman, 1981, Laboratory studies on natural gouge from the U.S. Geological Survey Dry Lake Valley No. 1 well, San Andreas fault zone, *in* N. L. Carter, M. Friedman, J. M. Logan, and D. W. Stearns, eds., Mechanical behavior of crustal rocks, the Handin volume: American Geophysical Union Geophysical Monograph 24, p. 121-134.

Murray, G. E., 1961, Geology of the Atlantic and Gulf coastal province of North America: New York, Harper Brothers, 692 p.

Pessagno, E. A., Jr., 1967, Upper Cretaceous planktonic foraminifera from the western Gulf coastal plain: Paleontographica Americana, v. 5, p. 245-445.

——— 1969, Upper Cretaceous stratigraphy of the western Gulf Coast area of Mexico, Texas, and Arkansas: GSA Memoir 111, 139 p.

Priest, S. D., and J. A. Hudson, 1976, Discontinuity spacings in rock: International Journal of Rock Mechanics, Mining Science and Geomechanical Abstracts, v. 13, p. 135-148.

Roemer, F., 1852, Die Kriedebildungen von Texas and ihre organischen einschluesse: Bonn, Adolpus Marcus, 100 p.

Scholle, P. A., and K. Cloud, 1977, Diagenetic patterns of the Austin Group and their control of petroleum potential, *in* D. G. Bebout and R. G. Loucks, eds., Cretaceous carbonates of Texas and Mexico, applications to subsurface exploration: University of Texas Bureau of Economic Geology Report of Investigations 89, p. 257-259.

Shimamoto, T., and J. M. Logan, 1981, Effects of simulated clay gouges on the sliding behavior of Tennessee sandstone: Tectonophysics, v. 75, p. 243-255.

Summers, R., and J. D. Byerlee, 1977, A note on the effect of fault gouge composition on the stability of frictional sliding: International Journal of Rock Mechanics, Mining Science and Geomechanical Abstracts, v. 14, p. 155-160.

Weeks, A. W., 1945, Balcones, Luling, and Mexia fault zones in Texas: AAPG Bulletin, v. 29, p. 1733-1737.

Young, K., 1963, Mesozoic history, Llano region, *in* V. E. Barnes, W. C. Bell, S. E. Clabaugh, P. E. Cloud, Jr., K. Young, and R. V. McGehee, eds., Field excursion: geology of the Llano region and Austin area: University of Texas Bureau of Economic Geology Guidebook 5, p. 98-106.

Younger, M. S., 1979, Handbook for linear regression: Belmont, California, Wadsworth, Inc., 385 p.